JP9.6 HOW TRMM PRECIPITATION RADAR AND MICROWAVE IMAGER RETRIEVED RAIN RATES DIFFER

Eun-Kyoung Seo[1*] and Guosheng Liu[2]
[1]Kongju National University, Kongju, chungnam, South Korea
[2]Florida State University, Tallahassee, Florida

1. INTRODUCTION

Main components of the Tropical Rainfall Measuring Mission (TRMM) microwave radiometer retrieval algorithm is to convert calibrated brightness temperatures (TBs) of the TRMM Microwave Imager (TMI) into attenuation/scattering indices and then invert the indices to rain rates using a coupled system of Bayesian theorem and the predefined database (Kummerow et al., 2000)]. The attenuation and scattering indices are vertically integrated properties. Meanwhile, the Precipitation Radar (PR) measures the intensity of backscattered energy from hydrometeors within a defined vertical interval; therefore, rain rates may be estimated at different altitudes. Since the active PR and passive TMI retrieval algorithms are based on different underlying principles, one retrieval can be used as a comparative reference for the other (Olson et al., 2006). It has been known that the zonally averaged TMI rain rates is 24% larger than the PR rain rates over tropical region for version 5 products (Kummerow et al., 2000). For the most up-to-date version 6 products, it is reported that the TMI surface rain rate has, in general, less bias with respect to independent estimates (Yang et al., 2006).

First, we examine how the TMI and the PR retrievals differ with respect to rain intensity and convective fraction using collocated pixel data over ocean. This exercise helps us understand what rain type/intensity causes the largest mismatch between the two retrievals. To get further insight of the mismatch, we then examine the TB - rain rate relations separately using PR- and TMI-derived rain rates as truth. This exercise sheds lights on why the mismatch occurs. Finally, we discuss the possible shortcomings of the TMI algorithm under the assumption that the PR retrievals better represent the truth.

2. DATA

Datasets used in this study are TRMM TMI TBs and the standard version 6 products of TMI-derived rain rates and PR-derived rain rates over oceanic regions. The data duration is one year from 1 December 2004 to 30 November 2005. The analysis of this study is conducted only to those oceanic pixels whose TMI-derived rain rates are greater than 0. TMI and PR pixels were collocated by averaging PR rain rates over a nominal footprint (14 x 14 km^2) of TMI. The convective areal fraction (*convF*) is defined as the ratio of the number of convective PR pixels (in the range of 200 ~ 291 of rain type in 2A23 products) to the total number of collocated PR pixels within the footprint. Based on the convF, rain pixels are classified into one of the following three categories:

$$\text{category} = \begin{cases} 1 & , \text{ if } \quad 0.7 < convF \le 1.0 \\ 2 & \quad\quad\; 0.3 < convF \le 0.7 \\ 3 & \quad\quad\; 0.0 \le convF \le 0.3 \end{cases} .$$

Namely, categories 1, 2 and 3 constitute mostly convective, mixed, and mostly stratiform (or non-convective) rain, respectively. Of all the collocated rainy pixels, 11.6% are classified as category 1 (mostly convective), 11.4% as category 2 (mixed) and 77.0% as category 3 (mostly non-convective)

3. SPECTRAL DIFFERENCE BETWEEN PR AND TMI RAIN RATES

Using all collocated rain pixels of the one year over ocean, we compared the TMI- and PR-derived rain rates; the averaged difference between TMI- and PR-derived rain rates in each 1 mm h^{-1} PR rain rate and 0.1 *convF* bin is plotted in Figure 1 along with frequency of occurrence of rain pixels in each bin. The magnitude and sign of the TMI minus PR rain rate present a distinct dependence on rain intensity, as well as on convective fraction to a less extent. TMI rain rates are higher than PR rain rates at low rain intensity while lower at high rain intensity; the transition from positive to negative difference occurs around 1 to 6 mm h^{-1} PR rain rate. On the other hands, given the same PR rain rate, the TMI rain rates are generally higher than the PR-derived rain rates when *convF* is low while lower when *convF* is high. The average difference of TMI minus PR rain rates are -2.287, -1.26 and 0.55 mm h^{-1}, for rain categories 1, 2, and 3, respectively

4. MULTIVARIATE RELATIONS OF RADIANCE INDICES TO RAIN RATES

The TMI algorithm uses attenuation (P) and scattering (S) indices defined by Petty (1994) instead of the nine TBs to estimate rain rates. The attenuation index (P) is a normalized polarization difference, ranging from 0 (opaque) and 1 (cloud-free). Another radiance index, scattering index S, represents volume scattering associated with frozen precipitation aloft. We modified the Petty's P and S slightly as follows. The new P is redefined as 100(1 - P') and the S is redefined as –S', where P' and S' are (1) and (2) in Petty (1994). Greater values of the new P and S correspond to larger liquid volume and smaller ice volume, respectively.

To simplify the representation of observed signatures while capturing the major features, in this study,

* *Corresponding author address:* Eun-Kyoung Seo, Kongju National University, Dept. of Earth Science Education, Korea, 314-701; email: ekseo@kongju.ac.kr.

Empirical Orthogonal Function (EOF) analysis for five radiance indices (i.e.: P10, P19, P37, P85, and S85; subscripts denote the frequency of TMI channels) is employed. The first and second EOF patterns represent a vertically-coupled tall and a liquid-dominant (or ice-dominant) cloud, respectively. Using the amplitudes of the two leading EOFs as abscissa and ordinate, we may plot the occurrence frequency of rain pixels and PR- or TMI-derived rain rates in EOF space (Figure 2).

The left panel of Figure 2 shows the frequency of rain pixel occurrence, mean rain rate derived from PR and mean rain rate derived from TMI for the category 1 (convective) rain events. While the increase of PR rain rates correspond to the increase of both the first and the second EOFs' amplitude, the high values of TMI-derived rain rate are clustered mostly at the lower-right corner of the diagram – highly positive for the first EOF amplitude and highly negative for the second EOF amplitude. This implies that for a high rain rate the PR retrieval corresponds to a rain profile of relatively balanced high-liquid and high-ice hydrometeor profile while the TMI retrieval corresponds to a hydrometeor profile with excessive ice (highly negative second EOF amplitude). If we assume that the PR retrievals are closer to the truth, this above inconsistency may point to a problem of the excessive ice hydrometeors in the predefined TMI algorithm database as discussed by Seo et al. (2007a). Furthermore, there is another significant difference: the TMI-derived rain rates (Figure 2g) in particular for heavy rain events are much smaller than PR-derived rain rates (Figure 2d). The TMI-derived mean rain rate does not exceed about 35 mm h^{-1}, while the PR-derived mean rain rate can be as high as 80 mm h^{-1}. If we assume that the PR retrievals are more close to the truth, the underestimation by TMI may be attributed to the following two problems: (1) the excessive ice hydrometeors in the predefined database, (2) inadequate treatment of the beam-filling problem, which is quite significant for TMI observations of convective rain events, and (3) the lack of high rain rates (> 60 mm h^{-1}) in the predefined database itself.

In category 3 (non-convective), the PR- and TMI-derived rain rates have similar range. However, the relationship between TMI radiance and rain rates has the similar trend to that for category 1. That is, the excessive ice hydrometeors in the predefined database seem to be problematic in high rain rates even for category 3. In low rain rate (< 10 mm h^{-1}) for category 3, the TMI rain rates are higher than the PR rain rates, which is largely responsible for overall positive difference of TMI minus PR rain retrievals because of the large population of pixels in this range. The possibilities can be as follows: (1) the insensitivity of the PR to rain rates lower than 0.7 mm h^{-1}, (2) the uncertainty in determining no-rain "background" TMI TBs, and (3) the lack of data points with zero rain rates in the predefined database of the Bayesian-type TMI retrieval algorithm. In relation to the last point, a realistic prior PDF having all zero rain rates as well as rain events might decrease the difference by lowering TMI rain rates in very light rain rate. Details can be found in Seo et al. (2007b).

5. CONCLUSIONS

It was found that for the collocated TMI and PR pixels there is a small positive difference (0.02 mm h^{-1}) between TMI- minus PR-derived rain rate. The slight difference is led by the cancellations between convective/mixed and non-convective categories and between lower-rate and higher-rate rain clouds. In particular, the convective rain clouds show negative while non-convective rain clouds show positive difference of TMI- minus PR-derived rain rates.

Using the corresponding relations between retrieved rain rates and the leading EOFs of observed TBs, we attempt to get further insight of the difference between the PR and the TMI retrievals. In the convective rain cloud category, TMI-derived rain rates are systematically lower than those derived by the PR when the attenuation and scattering signals become stronger. In the non-convective rain cloud category, TMI-derived rain rates are higher than the PR-derived ones when the attenuation and scattering signals are weak (rains are lighter), which is primarily responsible for the overall positive bias of the TMI- minus the PR-derived rain rates due to the large population of rain pixels in the rain rate range and category. At high rain rates of all the categories, high PR-derived rain rates correspond to strong attenuation and scattering microwave signatures, implying hydrometeor profiles of relatively balanced amount of both liquid and ice. In comparison, high TMI-derived rain rates correspond to excessive ice scattering microwave signatures.

REFERENCES

Kummerow, C. D., and Coauthors, 2000: The Status of the Tropical Rainfall Measuring Mission (TRMM) after Two Years in Orbit. *J. Appl. Meteor*., 39, 1965–1982.

Olson, W. S., and Coauthors, 2006: Precipitation and latent heating distributions from satellite passive microwave radiometry. Part I: Method and uncertainties. *J. Appl. Meteor. Climatol.,* 45, 702–720.

Petty, G. W., 1994: Physical retrievals of over-ocean rain rate from multichannel microwave imagery. Part II: Algorithm Implementation. *Meteorol. Atmos. Phys.*, 54, 101-121.

Seo, E.-K., G. Liu, W.-K. Tao, and S.-O. Han, 2007a: Adaptation of Model-Generated Cloud Database to Satellite Observations, *Geophys. Res. Lett.*, 34, doi:10.1029/2006GL027857.

____, G. Liu, and K.-Y. Kim, 2007b: A Note on Systematic Errors in a Bayesian Retrieval Algorithm, *J. Meteor. Soc. Japan*,, 85, 69-74.

Yang, S., and Coauthors, 2006: Precipitation and latent heating distributions from satellite passive microwave radiometry. Part II: Evaluation of estimates using independent data. *J. Appl. Meteor. Climatol.,* 45, 721–739.

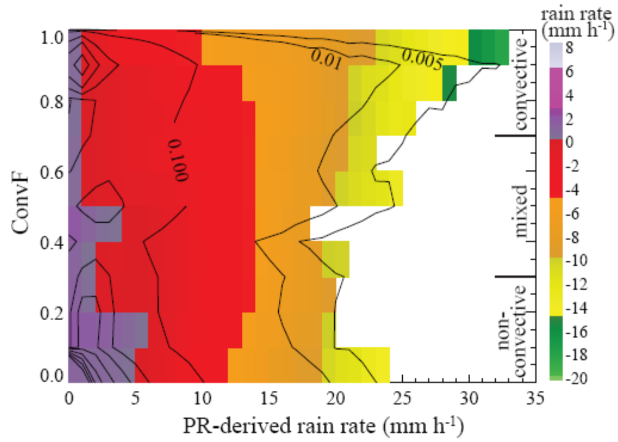

Figure 1. The difference (color pixels) in mm h^{-1} between TMI- minus PR-derived rain rate as a function of PR rain rate and *convF*. Contours represent occurrence frequency of rain pixels in % at the intervals of [0.005, 0.01, 0.1, 0.5, 1, 2, 4, 6, 8, 10].

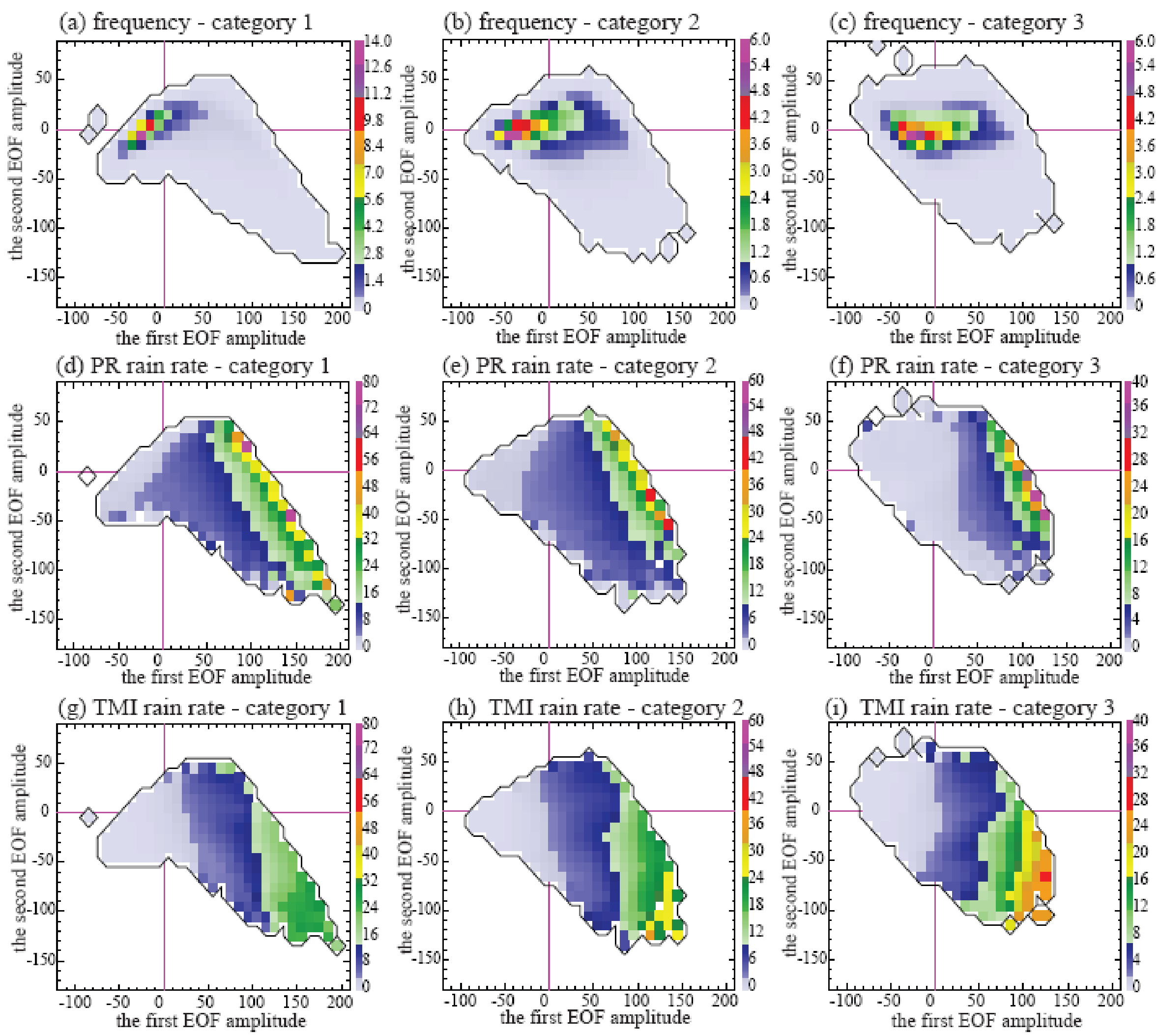

Figure 2. (a-c) occurrence frequency (%) of the two leading EOF amplitudes, (d-f) PR-derived rain rate (mm h^{-1}), and (g-i) TMI-derived rain rate (mm h^{-1}) in the EOF space.